NUMERICAL MODELING OF HYDROTHERMAL CONVECTION SYSTEMS INCLUDING SUPER-CRITICAL FLUID

Mineyuki Hanano[1] and Mohan S. Seth[2]

1) JMC Geothermal Engineering Co., Ltd.
72-2 Sasamori, Ukai, Takizawa-mura, Iwate 020-01, Japan
e-mail: hanano@geothermal.co.jp
2) Technical Software and Engineering, Inc.
2506 Springwood Lane, Richardson, TX 75082, **U.S.A.**
e-mail: mseth@metronet.com

key words: geothermal systems, hydrothermal systems, magma intrusion, natural convection, numerical modeling, super-critical fluid

Abstract

Development of deep geothermal resources exceeding 300°C has become very important in many geothermal fields. To adequately describe the entire picture of a total fluid circulation which is very important to understand the nature of such deep high-temperature geothermal resources, we have developed a numerical simulator capable of simulating geothermal reservoirs which may contain super-critical fluid, up to 800°C and 1000 bars. To overcome computational problems associated with rapid changes in fluid properties around and within a certain region above the critical point, we employed interpolation in the vicinity of the region. Using this simulator, we demonstrate that we are able to model deep hydrothermal convection systems.

INTRODUCTION

Natural convection is the most important mechanism to transport heat in currently developed geothermal systems. Natural state modeling is commonly employed to study such hydrothermal systems (e.g. Bodvarsson, 1988). Numerical natural-state models give valuable insight into mass and heat transfer in geothermal systems and also provide stable initial conditions for subsequent exploitation studies.

Recently, exploration and development of deep geothermal resources have become very important in many geothermal fields (e.g. Gianelli et al., 1988; Thompson, 1989; Reyes, 1990; Hanano and Takanohashi, 1993). In such geothermal fields, large bodies of very young intrusive rocks and high temperature reservoirs exceeding 300°C are found. One of the examples of such deep geothermal resources is Kakkonda, Japan (e.g. Hanano, 1995). In Kakkonda, there is a relatively low-permeability high-temperature reservoir of 350 to 360°C below about 1,500m depth, and a large body of neo-granitic pluton (Kakkonda Granite) of 0.34 to 0.07Ma was found from about 2,000 to 2,800m depth (e.g. Kato and Doi, 1993; Kanisawa et al., 1994). Similar conditions to Kakkonda, a permeable shallow reservoir at 250°C, a less permeable deeper reservoir at 350°C, hydraulic connection between the shallow and deep reservoirs, and a young pluton not far from the developed zone with metamorphic minerals such as biotite, were found in The Geysers, California (e.g. Walters et al., 1988).

To model the evolution process of the natural state of such high temperature reservoirs, we should account for the process of the onset and development of natural hydrothermal convection after the intrusion of such magmatic pluton. Such a magmatic pluton must have been 600 to 800°C when it was intruded. Such high temperatures suggest the occurrence and existence of super-critical fluid around the intrusive. The existence of super-critical fluid in the Nesjavellir geothermal field, Iceland has been reported by Steingrimsson et al. (1990). We also should account for total hydrothermal convection systems from a great depth, through reservoirs at exploitable depth, to the ground surface, to adequately describe the entire picture of total fluid circulation in geothermal systems.

There have been many efforts to simulate super-critical fluids (e.g. Norton and Knight, 1977; Cathles, 1977; Roberts et al., 1987; Cox and Pruess, 1990; Hayba and Ingebritsen, 1994). We have developed a numerical simulator to model high-temperature hydrothermal convection systems which may include super-critical fluid in the vicinity of the magmatic pluton and purely heat conductive cooling of the pluton. In this paper, we describe the numerical simulator and present an example of modeling of such a high-temperature hydrothermal system.

GENERAL DESCRIPTION OF THE SIMULATOR

All results presented here were obtained using Technical Software and Engineering's geothermal simulator known as SIM.FIGS (Fully Implicit Geothermal Simulator). SIM.FIGS is a general purpose three-dimensional model for mass and heat transfer in single- and multiple-porosity porous media, based on a fully-implicit (or optionally-sequential) finite-difference formulation. The model basically consists of two equations expressing conservation of mass of water/steam and conservation of energy in porous media. The equations and solution procedures are the same as those described by Coats (1977). The procedure employs a variable substitution approach, where pressure and temperature are chosen as the solution variables for single-phase water and steam, and pressure and saturation are chosen as those for two-phase water and steam. The matrix equations comprising of 2x2 unknowns per grid-block are optionally solved using the D4- ordered direct method (Price and Coats, 1973), the line successive overrelaxation method, or one of several preconditioning and acceleration schemes which employs the conjugate gradient type approach (Vinsome, 1976; Cheshire et al., 1980; Oppe et al., 1988) for nonsymmetrical matrices.

The model simulates thermal, viscous, gravity and capillary forces, taking into account reservoir heterogeneity, geometry, variation in fluid properties, a host of different production-injection schedules, surface separator, two-phase flow behavior in production wells, heat losses from the under-burden, over-burden and adjacent side strata, aquifer influx from the surrounding regions, and other pertinent factors. Additional capabilities of SIM.FIGS include the treatment of double porosity (fractured reservoirs) systems using Warren and Root type (e.g. Gilman and Kazemi, 1983) and Multiple Interacting Continua (MINC) concepts (Pruess and Narasimhan, 1985), and n-component flow (mass transport) suitable for tracer tracing applications; it has an efficient solution procedure for MINC flow (Seth and Hanano, 1995). The local grid refinement feature affords a more detailed resolution in the areas of interest. Heat transfer by conduction only, is considered for non-porous rock bodies. SIM.FIGS has been validated with several analytical results and also with the results of other reservoir simulators under subcritical conditions (e.g. Stanford Geothermal Program, 1980).

IMPROVEMENT OF THE SIMULATOR

We improved SIM.FIGS to treat super-critical fluid up to 800°C and 1000 bars. Our goal was to keep the method simple, computationally stable, and easy to implement into any existing geothermal simulator. **A** careful study of the fluid properties of pure H_2O reveals that there are two principal characteristics which pose computational problems:

(1) Fluid behavior around the critical point:

The properties change extremely rapidly in the vicinity of this region which renders the computational task highly unstable. Fluid saturations can undergo a change of 100% with a slight change in the temperature, pressure, or both.

(2) Rapid change in the properties across the subregions 2 and 3:

Sub regions identified as 2 and 3 in Fig.1 represent the region with the super-critical fluid (e.g. International Formulation Committee, 1967). The boundary denoted as β_L divides these two regions. There is a steep density gradient across this boundary with a much higher density in the region 3. Such a steep change in the density manifests itself in the form of a large pressure change as a point traverses across this boundary, which in turn limits the time step size in numerical simulation. Studying the natural state of high-temperature hydrothermal convection systems entails simulation periods of several tens of thousands to a few million years, a reasonably large time-step size (of the order of a few tens to a few thousand years) **is** a practical necessity.

Apart from the above complexities in the fluid properties, there is nothing in the basic mathematical formulation of **a** conventional geothermal simulator which limits its applicability in all pressure and temperature ranges.

To numerically simulate fluid flow, under such a thermodynamic condition, Cox and Pruess (1990) employed a two-dimensional table of densities and internal energies as functions of temperature and pressure in a critical region, from the formulation developed by Haar et al. (1984). They also employed a hi-linear interpolation schemes to estimate values between table values. On the other hand. Hayba and Ingebritsen (1994) used pressure and enthalpy as variables to facilitate computational problems caused at the critical point. They used a look-up table for density, viscosity and temperature as a function **of** pressure and enthalpy. They used a bi-cubic interpolation.

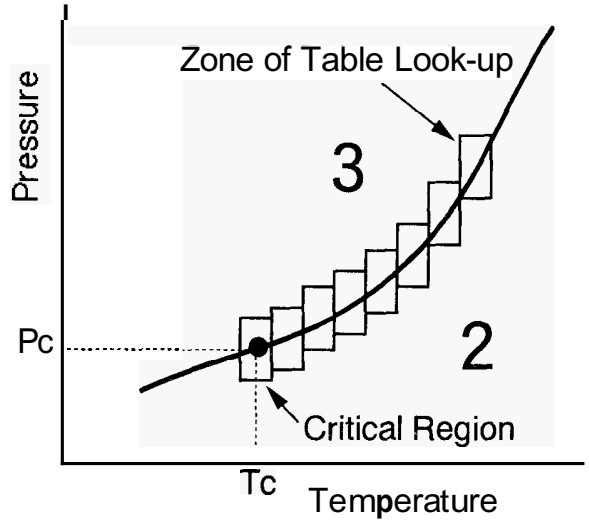

Fig.2 Illustration of zones of table look-up around the critical point. 2,3: Subregions shown in Fig.1. Tc, Pc: Critical temperature and pressure, respectively.

We employ a slightly different approach. We employ temperature and pressure as variables for the critical fluid like single-phase water and steam. However, the key clement of our approach lies in smoothing-out the severe discontinuities and steep density gradients in the phase envelope. We replace the true critical point at 374.15°C and 221.2 bars by a small rectangular "critical region" bounded by a rectangle which bounds 370 and 375°C, and 218 and 223 bars on the P-T diagram of water (Fig.2). The properties within the rectangle are determined by bi-linear interpolation of the values at the corners of the rectangle. The values at the corner are calculated by the correlations given by the International Formulation Committee (IFC) (e.g. International Formulation Committee, 1967). Within the critical region, the properties of water and steam arc taken to be identical and the relative permeability are assumed to be linear functions of saturations. In the coding logic, we treat this fluid in a manner similar to cases of single-phase water,

The densities and the internal energies of super-critical fluid in the vicinity of the boundary between the regions 2 and 3 are treated in an analogous manner as that around the critical point (Fig.2). We constructed a table of densities and internal energies with values calculated at $\{P(\beta_L)-\Delta P\}$ and $\{P(\beta_L)+\Delta P\}$ where AP is arbitrarily taken to be 3-5 bars. Beyond this $2\times\Delta P$ wide zone, the PVT properties were calculated directly from the IFC correlations or by a table look-up procedure. **As** expected, the table look-up procedure is considerably faster than the calculations using the correlations. For a rapid table look-up procedure, we used a fixed increment of 5°C for temperature and 5 bars for pressure in the super-critical region.

It is readily obvious that smearing the critical point to a small region as well as linear interpolation across the above discussed zone along the boundary between the regions 2 and 3, introduces certain errors in the solution. On the other hand, a larger region and wider zone greatly improves the computational stability and permits much larger time-step sizes. We have carried out limited numerical experimentation with different sizes of the critical region and the width of the zone, and observed that the results are marginally affected by taking zone width and the critical region smaller than the 5 bar and 5°C increment. On the other hand, the near-critical fluid gives very high heat transfer, because of high heat capacity and high mobility (e.g. Norton and Knight, 1977). Thus, this treatment may have a possibility to loose or poorly represent the high heat transfer effect. and may leads to a lower estimate of heat transport from a heat source. However, our objective is to model the entire picture of a total fluid circulation within high temperature hydrothermal systems that ranges from a few to several tens kilometers. Thus, most of the area to be modeled is occupied by the sub-critica! fluid (usually less than 360°C), and a distribution **of** the near-critical fluid should be very limited. Thus, we think the proposed approach may not give a significant error from such a viewpoint. We, therefore, believe that the approach is sound and practical.

To perform accurate numerical simulations, a code verification is very important. The original version of SIM.FIGS has been validated under conditions below the critical point, as described above. However, as described by Cox and Pruess (1990), it seems to date that no adequate experimental data is available for the code verification for the near-critical flow in porous media. Thus, the modified version of SIM.FIGS has not been verified yet above the critical point except for the conventional mass and energy balance checks. It is a very important task to be studied further.

AN EXAMPLE RUN

Our final goal of numerical modeling using the improved version of SIM.FIGS is to model the natural state of fluid circulation that includes heat conductive cooling of the magmatic intrusives following intrusion in order to understand the complete picture of the high temperature hydrothermal systems like Kakkonda. **As** a first step of such modeling, we employed a simplified symmetrical two-dimensional cross-sectional porous model for an example because of its simplicity. Fig.3 shows its grid mesh, permeability distribution and bottom-boundary temperature distribution. To account for deep fluid circulation, we chose the depth and horizontal length of the model to be 6km and 18km, respectively. The thickness of the cross section was Ikm. Permeability distribution was basically two-layered, a relatively permeable shallow layer and a less permeable deep layer, based on the above-mentioned permeability structure of Kakkonda, Japan. All runs were carried out on a PC486/66 and Sun Sparc Station 2 and 5 computing systems.

Boundary conditions at both sides were closed to mass and energy. A boundary condition at the top surface was permeable and heat conductive, *i.e.* it was open to mass and energy with a constant temperature, 1°C and constant pressure, 1 bar. The bottom boundary was closed to mass but was heat conductive at a constant temperature as shown in Fig.3. Since, no mass and heat input were imposed from outside of the model, the system was heated by an intrusive of 800°C at the deep left comer (Fig.3) and by the bottom boundary.

The initial condition was static with linear temperature distribution, 15°C at the top surface and 600°C at the bottom, excluding the intrusive; the temperature of the entire intrusive was 800°C. The initial pressure was 1bar at the surface with a hydrostatic profile which corresponded to the initial temperature field. Therma! conductivity and rock heat capacity were 2W/m·K and 2.6MJ/m^3·K, respectively throughout the model. Porosity of the model was 10% excluding the intrusive. We assumed both porosity and permeability of the intrusive to be zero.

We ran the model up to 90,000 years. Changes of mass and heat in-place in the model over 90,000 years are shown in Fig.4. As seen in Fig.4, the heat in-place of the whole system once increased until 10,000 years due to heat gain by hcat conduction from the bottom boundary, and then it decreased due to thc out-flow of hot fluid and an in-flow of cold surface water to and from thc surface. The mass change is inversely proportional to the change of heat in-place. The mass and heat changes approached a quasi-steady state at around 40,000 years, though there still remained a small fluctuation.

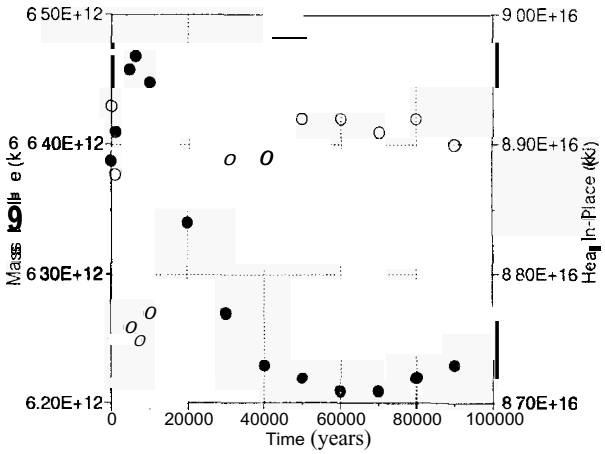

Fig.4 Changes of mass in-place (O) and heat in-place (O).

Fig.5 shows the cross-sectional temperature distribution at **10,000** years. As seen in Fig.5, convective hot up-flow develops at around X=4 and 5 (horizontal node number; around 1.8km to the right, from the **upper** left corner; c.f. Fig.3). **Also,** convective down-flow is notable at around X=1 and 2 (0 to 0.6km to the right from the upper left corner). This pair of convective up-flow and down-flow forms a local hydrothermal convection. Fig.6 is a temperature profile at X=5 (1.8km to the right from the upper left comer) above 3km depth. As seen in Fig.6, there are two temperature layers of approximately 250°C in thc shallow **zone** and approximately 350°C in the deeper zone. Thus, a two layered temperature structure perfectly similar to the situation of the shallow and deep reservoir in Kakkonda, Japan (e.g. Hanano and Takanohashi, 1993; Hanano, 1995) is well reproduced. This implies that the model may be representative of a real high temperature geothermal reservoir.

Fig.7 shows the cross-sectional temperature distribution at 90,000 years. In Fig.7, convective up-flow is seen at around X=3 and 4 (around 1.4km to thc right from thc upper left corner), and convective down-flow is **seen** at around X=1 (0 to 0.4km to the right from thc upper left corner), and X=7, 8 and 9 (around 3.2km to the right from the upper left corner). Also, the low permeability area from X=14 to 22 (9 to 18km to the right from the upper left comer) serves as the areal recharge **zone,** *i.e.* an areal convective down-flow zone. though its descending velocity is very small. Thus, there developed several roles of relatively small scale hydrothermal convection and one role of large scale hydrothermal convection to great depth. Super-critical fluid was widely present below 3.5km depth.

Another notable point in Fig.7 is the cool down of the intrusive. The intrusive at X=1 to 4 (0 to 1.6km to the right from the upper left comer) and Z=7 to 12, (vertical node number; 3 to 6km depth; c.f. Fig.3) which was originally 800°C at the start of the run, cooled down to the order of 400-700°C; its temperature was much lower than that in 10,000 years (c.f. Fig.5).

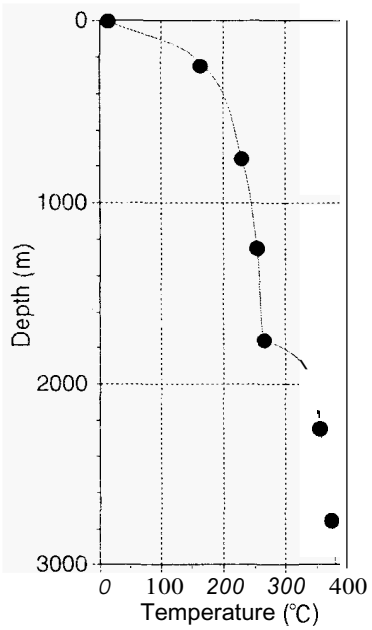

Fig.6 Temperature profile at X=S at 10,000 years. O: Simulated data.

As shown above, this example run demonstrates that we are able to model the total picture of an extensive hydrothermal convection system including super-critical fluid. The system inciudes not only the evolution process of the natural state of deep high-temperature hydrothermal convection systems which may contain super-critical fluid but also thermal structure and purely heat conductive cooling of intruded magma chambers. Therefore, the enhancements made to SIM.FIGS are useful not only for geothermal studies but also for volcanological studies, though there still remains the code verification above the critical point.

CONCLUSIONS

We have developed a numerical simulator capable of simulating geothermal reservoirs which may contain super-critical fluid up to 800°C and 1000bars, to study deep high-temperature geothermal resources. To overcome computational problems associated with rapid changes in fluid properties around and within a certain region above the critical point, wc employed interpolation in the vicinity of the region. The example run clearly demonstrates that we are able to model not only the total picture of the natural state of deep high-temperature hydrothermal convection systems but also thermal structure and purely heat conductive cooling of high-temperature magma intrusives.

Acknowledgement

The first author (MH) is grateful to the management of JMC Geothermal Engineering Co., Ltd. for their permission to publish this paper. The authors would like to thank the anonymous referee for helpful suggestions.

REFERENCES

Bodvarsson, G.S. (1988) Reservoir development strategy for hot water reservoirs with emphasis on reservoir modeling. *Bull. Geotherm. Resour. Council,* Vol.17, No.4, pp.69-YO.

Cathles, L.M. (1977) An analysis of the cooling of intrusives by ground-water convection which includes boiling. *Econ. Geol.*. Vol.72, pp.804-826.

Cheshire, I.M., Appleyard, J.R., Banks, D., Crozier, R.J. and Holmes, J.A. (1980) An efficient fully implicit simulator. *paper EUR-179 presented at EUROPEC 80 Conference, London, 1980.*

Coats, **K.H.** (1977) Geothermal reservoir modeling. *paper SPE-6892 presented at the 52nd Annual Fall Technical Conference of Society of Petroleum Engineers, Denver, Oct. 9-12, 1977.*

Cox, B.L. and Pruess, K. (1990) Numerical experiments on convective heat transfer in water-saturated media at near-critical conditions. *Trans. Porous Media,* Vol.5, pp.299-323.

Gianelli, **G.,** Puxeddu, M., Batini, F., Bertini, G., Dini, I., Panderi, E. and Nicolich, R. (1988) Geological model of a young volcano-plutonic system: the geothermal region of Monte Amiata (Tuscany, Italy). *Geothermics,* Vol.17, No.5/6, pp.27-36.

Gilman and Kazemi (1983) Improvements in simulation of naturally fractured reservoirs. *Soc. Pet. Eng. J.,* August 1983, pp.69.5-707.

Haar, L., Gallagher, J.S. and Kell, G.S. (1984) *NBS/NRC Steam Tables.* Hemisphere Publishing.

Hanano, M. (1995) Hydrothermal convection system of the Kakkonda geothermal field, Japan. *World Geothermul Congress, 1995, Florence, Italy.*

Hanano, M. and Takanohashi, M. (1993) Review of recent development of the Kakkonda deep reservoir, Japan. *Proc. 18th Workshop Geotherm. Res. Eng.,* Stanford Univ., pp.29-34.

Hayba, D.O. and Ingebritsen, S.E. (1994) Flow near the critical point: examination of some pressure-enthalpy paths. *Proc. 19th Workshop Geotherm. Res. Eng.,* Stanford Univ., in press.

International Formulation Committee (1967) *A Formulation of the Thermodynamic Properties of Ordinary Water Substance.* IFC Secretariat, Dusseldorf, Germany.

Japan Society of Mechanical Engineers (1981) *1980 SI JSME Steam Tables.* Japan Society of Mechanical Engineers, 124pp.

Kanisawa, **S.,** Ishikawa, K., Doi, N. and Kato, **O.** (1994) Neo-granitic pluton at the Kakkonda geothermal field, northeast Japan: Petrological characteristics of the quaternary pluton as the heat source. *Abstract, 16th General Meeting, International Mineralogical Association, Pisa, Italy, 1994.*

Kato, O. and Doi, N. (1993) Neo-granitic pluton and later hydrothermal alteration at the Kakkonda geothermal field, Japan. *Proc. 15th NZ Geotherm. Workshop,* Auckland Univ., pp.155-161.

Norton, D. and Knight, J. (1977) Transport phenomena in hydrothermal systems: cooling plutons. *Am. J. Science,* Vol.277, pp.937-981.

Oppe, T.C., Joubert, W.D. and Kincaid, D.R. (1988) *NSPCG User's Guide.* Center for Numerical Analysis, University of Texas, Austin, Texas.

Price, H.S. and Coats, K.H. (1973) Direct methods in reservoir simulation. *paper SPE-4278 presented at the 3rd SPE Symposium on Numerical Simulation, Houston, Jan. 11-12, 1973.*

Pruess, **K.** and Narasimhan (1985) A practical method for modeling fluid and heat flow in fractured porous media. *Soc. Pet. Eng. J.,* February 1985, pp.14-26.

Reyes, A.G. (1990) Petrology of Philippine geothermal systems and the application of alteration mineralogy to their assessment. *J. Volc. Geotherm. Res.,* Vol.43, pp.279-309.

Roberts, P.J., Lewis, R.W., Carradori, G. and Peano, A. (1987) An extension of the thermodynamic domain of a geothermal reservoir simulator. *Trans. Porous Media,* Vol.2, pp.397-420.

Seth, M.S. and Hanano, **M.** (199.5) *An* efficient solution procedure for multiple interacting continua flow. *World Geothermal Congress, 1995, Florence, Italy.*

Stanford Geothermal Program (1980) *Proc. Special Panel on Geothermal Model Intercomparison Study.* SGP-TR-42, Stanford Univ., 120pp.

Steingrimsson, B., Gudmundsson, A., Franzson, H. and Gunnlaugsson, E. (1990) Evidence of a super critical fluid at depth in the Nesjavellir field. *Proc. 15th Workshop Geotherm. Res. Eng.,* Stanford Univ., pp.81-88.

Thompson, R.C. (1989) Structural stratigraphy and intrusive rocks at The Geysers geothermal field. *Trans. Geotherm. Resour. Council,* Vol.13, pp.481-485.

Vinsome, P.K.W. (1976) Orthomin, an iterative method for solving sparse sets of simultaneous linear equations. *paper SPE-5729 presented at the 4th SPE symposium on Numerical Simulation, Los Angeles, Feb. 1976.*

Walters, M.A., Sternfeld, J.N., Haizlip, J.R., Drenick, A.F. and Combs, J. (1988) **A** vapor-dominated reservoir exceeding 600°F at The Geysers, Sonoma county, California. *Proc. 13th Workshop Geotherm. Res. Eng.,* Stanford Unit., pp.73-81.

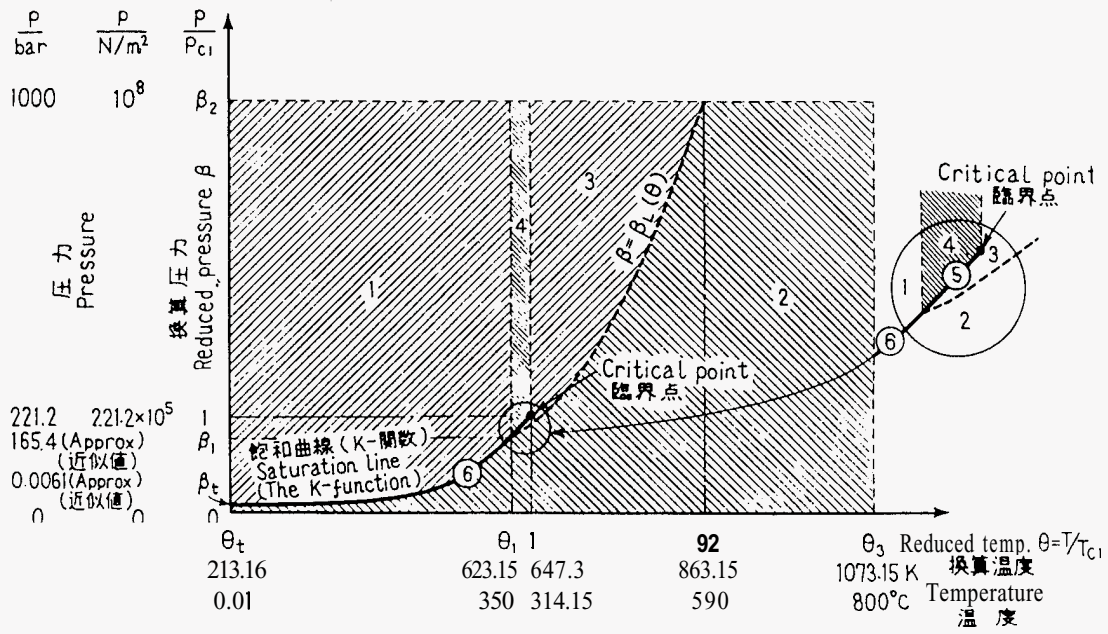

Fig.1 Illustration of subregions on the pressure–temperature diagram (Japan Society of Mechanical Engineers, 1981).

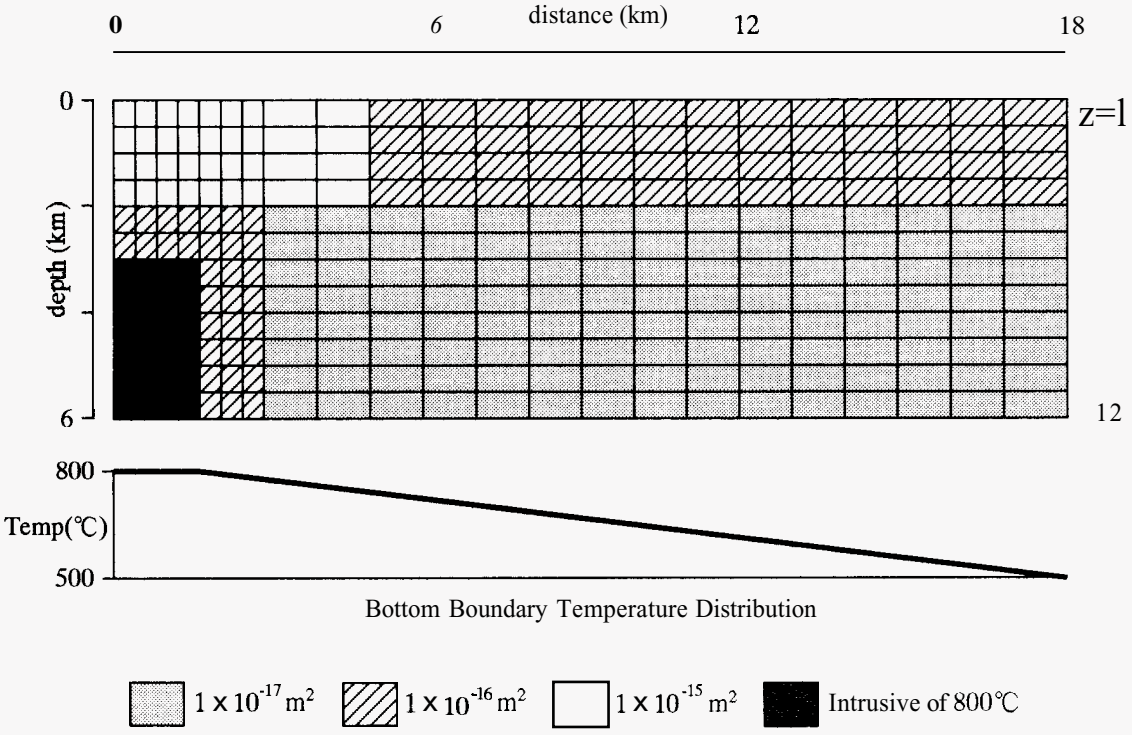

Fig.3 Grid mesh, permeability distribution and bottom boundary temperature distribution.

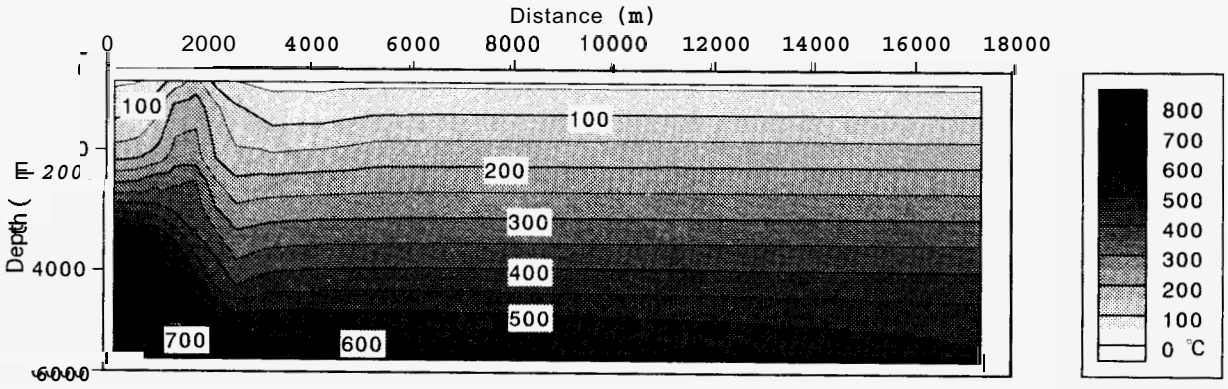

Fig.5 Temperature distribution at 10,000 years

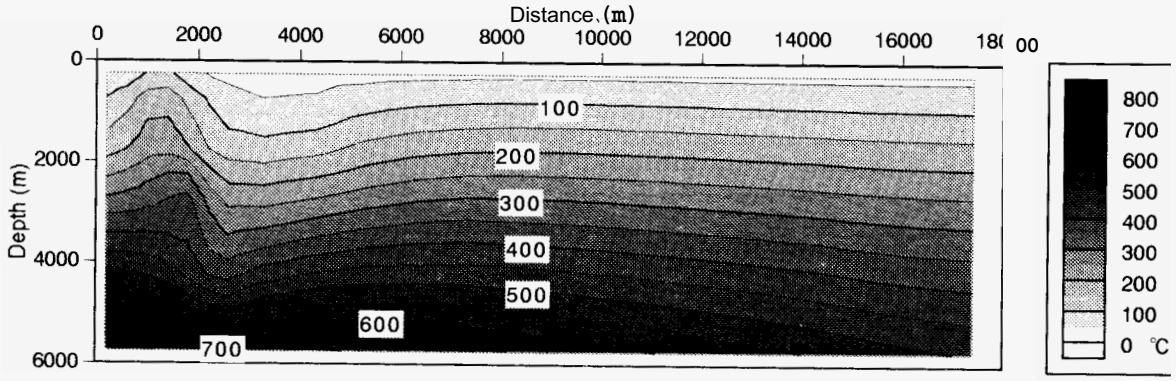

Fig 7 Temperature distribution at 90,000 years.